This is a preprint, the final version is subject to change, of the American Mineralogist (MSA)
Cite as Authors (Year) Title. American Mineralogist, in press.
(DOI will not work until issue is live.) DOI: http://dx.doi.org/10.2138/am-2016-5537CCBYNCD

Revision 1

An advanced rotational rheometer system for extremely fluid liquids up to 1273 K and applications to alkali carbonate melts

Danilo Di Genova[1], Corrado Cimarelli[1], Kai-Uwe Hess[1], Donald B. Dingwell[1]

[1]Department of Earth and Environmental Sciences, Ludwig-Maximilians-Universität München, Theresienstrasse 41/III, 80333 Munich, Germany

* Corresponding author

Danilo Di Genova

e-mail: danilo.digenova@min.uni-muenchen.de

Tel.: +498921804218

Fax: +498921804176

ABSTRACT

A high temperature rheometer equipped with a graphite furnace, characterized by an air-bearing-supported synchronous motor, has been enhanced by a custom-made Pt-Au concentric cylinder assembly. With this adaptation, viscosity measurements of highly fluid melts can be achieved at high temperatures, up to 1273 K.

Due to the air-bearing-supported motor, this apparatus can perform measurements of extremely low torque ranging between 0.01 μNm and 230 mNm (resolution of 0.1 nNm), extending the typical range of viscosity measurements accessible in the present configuration to $10^{-3.5}$ - $10^{3.5}$ Pa · s and shear rates up to 10^2 *(OM)* of sec^{-1}.

We calibrated the system with distilled water, silicone oils and the DGG-1 standard glass. We further present new data for the viscosity of Na_2CO_3, K_2CO_3 and Li_2CO_3 liquids. Finally, a comparison between our results and literature data is provided, in order to illustrate the effect of chemical composition and oxygen fugacity on the viscosity of alkali carbonate melts, which serve as analogs for both volcanic melts and molten systems of industrial relevance.

This study substantially improves the database of alkali carbonate melts and dramatically increases the accuracy of previous measurement attempts. The very low viscosity range data and the temperature-dependence also constrains very well the activation energy of these highly fluid systems and confirms the estimate of the pre-exponential factor for non-Arrhenian viscosity-temperature relationships.

Keywords: viscosity, highly fluid melts, carbonatite, alkali carbonate melts, molten carbonate fuel cells, MCFCs, high-temperature rheometry

INTRODUCTION

Viscosity is a fundamental property influencing the fluid dynamics of natural and synthetic systems. In recent years, the mobility of naturally-occurring and extremely fluid, carbonatite melts, has attracted renewed interest (Liu et al. 2007; Jones et al. 2013 for a review). Such melts are considered to be the main transport agent of carbon from the mantle to the crust and are thought to be intimately linked to the generation and transport of kimberlites to the Earth´s surface (Russell et al. 2012).

Due to the extremely low viscosity of these melts and their near ubiquitous presence in the asthenosphere, carbonatite melts may play a crucial role in the relative motion of tectonic plates, hence in the shaping of the Earth's crust (e.g. Hammouda and Laporte 2000; Gaillard et al. 2008). Gaillard et al. (2008) proposed that high conductivity values obtained for the asthenosphere would indicate the presence of small but significant amounts of carbonate melt in the upper mantle.

From a planetary perspective carbonatite melts are believed to be involved, as erosive fluids, in the formation of lava channels and valleys observed on Venus (Baker et al. 1992; Kargel et al. 1994; Treiman 1995). The astonishing lengths of channel landforms (up to 6800 km) and their fluvial-like shape, together with their longitudinal continuity, suggest that Venusian lavas may have been characterized by extremely low viscosities. As carbonatites are almost exclusively associated with alkali mafic and ultramafic silicate melts on Earth (Baker et al. 1992 and references therein, Russell et al., 2012), the two ultra-mafic and highly-potassic compositions (Venera 8 and 13 probes, see Treiman 1995, and references therein) measured *in-situ* in the Venera 13 sample

(nephelinite) and by the Vega rover (Soviet Venera and Vega programs, 1981/5) provide strong support for the presence of carbonatite melts on Venus.

Beyond their geologic and planetary science importance, carbonate melts are assuming an increasingly important role in industrial processes. Lithium-, potassium- and sodium- carbonate melts are employed as electrolytes in molten carbonate fuel cells (MCFCs), which operate at high temperatures (~923 K), for the production of CO_2-emission-free electricity. For this reason MCFCs are considered one of the most promising sources of green power production in the near future (Koishi et al. 2000). However, it has been demonstrated that the physical properties of molten alkali carbonates employed in the MCFCs affect the cell performances and durability (Reeve and Tseung 1996 and references therein; Yoshiba et al. 2004). Consequently, a detailed knowledge of the physical properties of molten alkali carbonates assumes a strategic importance in view of future improvements and electricity generation capabilities.

It is therefore evident that accurate measurement of flow properties and in particular the liquid viscosity is key to modeling the mobility of carbonate melts both in nature and in industrial and technological processes.

Obtaining accurate viscosity measurements of these extremely fluid melts involves several serious experimental challenges due to their high volatility, corrosive action on crucible materials, as well as the very low torques to be expected in this viscosity range.

To overcome these experimental limitations, we have customized a low-torque and high-temperature commercial rheometer system to enable measurements on extremely low viscosity melts. Here we present the calibration of the rheometer together

with the results of a viscosity study of different alkali carbonate melts, as a function of temperature and oxygen fugacity at ambient pressure. We compare the obtained results with literature values and discuss the effect of chemical composition on the viscosity behaviour.

INSTRUMENT DESCRIPTION

The measuring device consists of a controlled stress and strain rheometer, incorporated air bearing-supports, and an electronically commutated (EC) synchronous motor. Fig. 1 shows the apparatus together with an illustration of both the synchronous-electronically-commutated (EC) motor and the measuring geometry used in this study.

In contrast to traditional controlled-strain rheometers involving rotational variable displacement transducers (e.g., Dingwell 1986), here the electrical current of the motor is used as the measure of the torque. For this reason, a separate transducer measuring the torque is obviated and the measured value is not influenced by the torque needed to accelerate the motor (Läuger and Stettin 2010). The rheometer is air- and water-cooled to protect and stabilise the electronics. All these features taken together yield rheological measurements with unprecedented accuracy and precision.

Additionally, the motor, which is equipped with a permanent magnet on the rotor, is defined as a synchronous motor because the magnetic field in the stator rotates always at a speed proportional to the frequency of the applied voltage. This configuration allows the maintenance of constant motor characteristics, which prevents any drift of the registered signal and excludes any change in the relation between the applied electrical current to the motor and the measured torque. This feature represents one of the main

advantages of a synchronous motor in respect to classical drag-cup motor in performing rheological measurements (Läuger and Stettin 2010).

Another peculiarity of the EC motor lies in the absence of mechanical contacts to excite the motor. In comparison with motors involving brush contacts to activate the rotor, this contactless solution provides several advantages, including: i) a higher reliability and lifetime of the motor, ii) a reduction of noise and iii) an overall reduction of electromagnetic interference.

Using the apparatus presented in this work it is possible to perform viscosity measurements characterized by very small torques of less than 0.5 mNm (which is typically taken to be the lower limit of common mechanical commutation rheometers). At the same time, this setup allows applying high torques (up to 230 mNm) for long times, thus enabling a continuous and wide dynamic range of measurements.

In order to perform viscosity measurements at high temperatures (up to 1273 K) without the threat of reaction of sample with the viscometer materials, custom-made Pt-Au crucible and spindle have been fabricated (Fig. 1) replicating the original geometry made out of steel. The measuring geometry consists of a concentric cylinder arrangement, where the outer cylinder has a diameter of 24 mm and the gap between the two cylinders is 1 mm. The furnace is an electrical resistance “convection temperature device” (CTD 1000), mounting a K type thermocouple positioned at the base of the measuring cup. The chamber is cooled by water, while the sample is heated by convection and radiation of heat produced by the heating elements. Finally, the geometry of the furnace is such to allow for viscosity investigation under controlled gas flows including gas mixtures, such

that partial pressures of active chemical components (e.g. oxygen fugacity) can be controlled.

INSTRUMENT CALIBRATION

The instrument was calibrated in a broad viscosity (η)-shear rate ($\dot{\gamma}$)-temperature (T) interval. In particular, 53 calibration measurements were performed in the temperature range from 293 to 1273 K, at standard viscosity ranging between -3.33 and 3.13 log Pa · s, and shear rates from 0.5 to 70 sec^{-1} and using both the steel and Pt-Au assemblies. For the calibration both the steel and the Pt-Au assemblies were used. The investigated η-$\dot{\gamma}$-T interval well overlaps with the interval relevant for volcanological and industrially interesting carbonate and carbonatitic melts. For example, Norton and Pinkerton (1997) performed viscosity measurements of carbonatites from Lengai volcano (Tanzania) in the temperature range 773 to 923 K, applying different shear rates up to 30 sec^{-1}. The measured viscosity ranged between 0.15 and 260 Pa · s.

The standard materials we used for the calibration are 1) distilled water, 2) a Newtonian silicone oil (viscosity standard Cannon N15000) and 3) a soda-lime-silicate viscosity standard glass (DGG-1, supplied by the *Deutsche Glastechnische Gesellschaft*). Using DGG-1, we additionally check for thermal gradient along the crucible and/or shear heating effect. The absolute error in temperature derived from the high-precision viscosity measurements is less than 3 K, therefore we consider this effect negligible.

The calibration results are reported in Tab. 1 together with the certified viscosity values of the standards. The standard materials have been chosen to cover a wide range of

159 viscosities and temperatures against which the rheometer, equipped with both steel and
160 custom-made measurement geometries has been calibrated.

161 The measured viscosities for distilled water (using the steel assembly) are shown
162 in Fig 2a as a function of time, temperature and shear rate. These measurements were
163 performed at 303 and 333 K and at shear rates of 30, 50, 60 and 70 sec^{-1}. The measured
164 viscosities range between -3.33 and -3.09 log Pa · s, (0.463 to 0.807 mPa · s),
165 respectively.

166 Before starting the viscosity measurement, the distilled water was stirred for 5
167 minutes in order to achieve thermal equilibrium of the entire system (water + steel
168 assembly). Additionally, due to the rapid water evaporation, the viscosity at the 333 K
169 was measured at time intervals of 1 minute, whereas at 303 K the viscosity was measured
170 every 5 minutes. Measured viscosities at 333 K (Fig. 2a) are more scattered with respect
171 to those at 303 K. This is because the sampling rate (1 min) at 333 K is probably too short
172 to obtain a stable value of viscosity. Despite the slight data scattering, the results match
173 very well the reference values of viscosity of distilled water at 333 K (Tab. 1). In order to
174 test the reproducibility of our results, the measurements were repeated 5 times. The
175 precision in measuring the viscosity of water ranges between 0.001 and 0.008 log Pa · s,
176 which corresponds to 0.3 and 1.9%, respectively.

177 Viscosity measurements of the Newtonian silicone standard (Cannon N15000)
178 were carried out at 298, 313, 323, 333, 353 and 373 K by using the Pt-Au spindle and
179 cup. The viscosity was measured at each temperature with 10 seconds sampling interval
180 for 5 minutes after waiting 10 minutes for thermal equilibration of the system. Moreover,

the reproducibility of our results was successfully verified by performing new viscosity measurements decreasing the temperature from 373 to 298 K (see Tab. 1).

Viscosity measurements have been performed as a function of temperature at different shear rates (5, 10 and 15 sec^{-1}) showing values ranging between -0.42 and 1.58 log Pa · s. The results are reported in Tab. 1 and shown in Fig. 2b as a function of time, temperature and shear rate. As expected, viscosity decreases from 298 to 373 K and the silicon standard exhibits a Newtonian behavior over the entire interval of temperature and shear rate investigated. These results are in perfect agreement with the references values, within ± 0.01 log Pa · s.

Additionally, we also considered the possibility of viscous heating due to the very high shear during viscosity measurements. The results showed that at high shear rate (100 sec^{-1}) and at 15, 20, and 40°C a viscous heating effect was detected after few minutes (i.e. an increase in temperature in the order of 0.2°C and a decrease in viscosity). For this reason those viscosity measurements were not taken into account for the calibration of the instrument.

Finally, the calibration of our device was augmented by performing high temperature measurements on the DGG-1 soda-lime silicate standard glass. Initially, a bubble-free glass was synthesized by melting the DGG-1 at 1773 K for 12 hours in the Pt-Au cup using a Nabertherm box furnace. Afterwards, the bubble-free glass was remelted in the rheometer furnace and heated to the target temperature. Finally the spindle was immersed in the sample to the measuring position and allowed to thermally equilibrate before starting the measurement. Viscosity measurements were carried out at 1273 K, the maximum temperature achievable with the rheometer furnace, for 80 minutes

at two different strain rates: 2.5 and 0.5 sec^{-1}. The average measured viscosity is 3.15 (±0.02) log Pa · s, while the reference values is 3.17 log Pa · s (Tab. 1).

Fig. 3 shows a comparison between the measured and the reference values. The large data symbols span the error of the measurements and the 1:1 linear regression agrees to within 0.004, 0.01 and 0.02 log unit for distilled water, silicone oil standard and DGG-1, respectively.

To summarize, the calibration validates the use of this new rheometer for viscosity measurements characterized by a high precision and accuracy. The measurements can be carried out between ambient temperature and 1273 K, in a viscosity range between -3.5 and 3.5 log Pa · s.

VISCOSITY MEASUREMENTS OF Na_2CO_3, K_2CO_3 AND Li_2CO_3

As noted above, the viscosity of molten carbonates is of great importance in both earth sciences and industrial processes. Notwithstanding their great importance, knowledge of the physical properties of these melts is still far from complete, with many of the available results being inconsistent having been apparently compromised by experimental complications.

Janz and Saegusa (1963), Vorob'ev et al. (1966) and Sato et al. (1999) have investigated the viscosity of lithium, sodium and potassium carbonate melts at/or near ambient pressure. Sato et al. (1999) reported a comparison between the results obtained from the different studies. According to these studies, within the investigated interval of temperature (1016 - 1234 K), Li_2CO_3, Na_2CO_3 and K_2CO_3 melts exhibit Arrhenian behavior.

227 Additionally, the viscosity data presented in Sato et al. (1999) and Vorob'ev et al.
228 (1966) are in good agreement, whereas a large discrepancy with the Janz and Saegusa
229 (1963) is observed.

230 Sato et al. (1999) observed a trend amongst the measured viscosities of the alkali
231 carbonate melts, in which the viscosity appears to be directly related to the ionic radius of
232 the cations. Nevertheless, the authors claim that two observed phenomena are difficult to
233 explain; 1) the reversal relation between the Rb_2CO_3 and K_2CO_3 viscosity and ionic
234 radius and 2) the similarity of viscosities of Li_2CO_3 and Na_2CO_3 melts.

235 We therefore performed viscosity measurements of Na-, K- and Li-carbonate (Fig.
236 4) to clarify the question of the relative viscosities of these melts and the validity of the
237 relationships presented in Sato et al. (1999). Firstly, in order to verify the chemical
238 stability of the carbonatite melts (e.g. decarbonization reactions), and the reproducibility
239 of measurements, the first measurement was performed at the highest temperature and
240 further measurements followed at 10 K intervals separated by cooling stages at 5 K min^{-1}.
241 The system was held at each temperature for enough time to obtain a stable value of
242 viscosity (i.e. minutes). Later, repeated viscosity measurements were performed at
243 temperature equal or very similar to the initial one. The comparison between the initial
244 measurements (during heating) and the last measurements (after cooling) shows no
245 changes of measured viscosity (see Table 2), indicating negligible influence of
246 decarbonization reactions on the viscosity measurements.

247 Viscosity measurements of Na_2CO_3, K_2CO_3 and Li_2CO_3 melts [from Merck,
248 purity $\geq$ 99.9% (Na_2CO_3), $\geq$ 99.5% (K_2CO_3) and $\geq$ 99.0% (Li_2CO_3)] were next carried
249 out in the temperature range of 1013-1213 K applying a shear rate of 20 sec^{-1}. The results

250 are reported in Tab. 2 and shown in Fig. 4 as a function of reciprocal absolute
251 temperature. The measured viscosities range between 3.6 and 14.2 mPa · s, and are
252 reported in Fig. 4 together with a comparison with the results of Sato et al. (1999) and
253 Janz and Saegusa (1963). Moreover, our samples show absolute viscosities which are in
254 good agreement with those reported in Sato et al. (1999) and Vorob'ev et al. (1966) (see
255 Fig. 3 in Sato et al. 1999), while those measured by Janz and Saegusa (1963) are
256 systematically lower than those reported here and in Sato et al. (1999).
257 Our data exhibit Arrhenian behavior over the investigated interval of temperature,
258 in accordance with the findings of Janz and Saegusa (1963) and Sato et al. (1999).
259 As data points follow an Arrhenian behavior, the measured viscosities can be
260 parameterized according to the following Arrhenian viscosity–temperature relationship:
261
262 $$\log \eta = A + \frac{B}{T} \qquad (1)$$
263
264 where η is the viscosity in Pa· s and T the absolute temperature. The fitting
265 parameters are reported in Tab. 3. Using this equation it is also possible to calculate the
266 activation energy of viscous flow [E_a, Tab. 3].
267 Calculated activation energies (27, 28 and 35 kJ mol^{-1} for K-, Na- and Li-
268 carbonate respectively) are comparable to those reported by Sato et al. (1999) and other
269 molten salts (Fig. 6 in Sato et al. 1999), while a big discrepancy can be observed with
270 data reported by Janz and Saegusa (1963). Indeed, data from Janz and Saegusa (1963)
271 show systematically higher activation energy of 70.71, 107.53 and 121.75 kJ mol^{-1} for Li-
272 , Na- and K-carbonate respectively.

In the case of molten salts (where measurement of very low viscosities is possible) the A parameter of Eq. 1 (the extrapolated viscosity at infinite temperature) could be linked to a minimum relaxation time (for gases and liquids) via the Maxwell relation ($\eta = G_\infty \cdot \tau_S$; ; where G_∞ is the shear module at infinite high frequencies and τ_S is the shear relaxation time). The physical interpretation of the minimum relaxation time is that of an average period of vibration of the liquid quasi-lattice of about $10^{-13.5}$ s. This minimum relaxation time (in a first approximation) is supposed to be independent from the composition of a liquid (Schmidtke et al., 2015). Angell (1989) found extrapolated viscosity data at infinite temperature for a wide range of chemical compositions (from oxides, silicates, metals to molten salts) varying only between -5 and -3 log η (Pa · s). Further, Russell et al. (2003) confirmed these values based on silicate melt compositions.

Values of the A parameter (Tab. 3) determined in this study vary between -3.8 and -3.1 log η (Pa · s); well within the values given by Angell (1989). On the contrary, the measured viscosities from Janz and Saegusa (1963) extrapolate to a range between -7.9 and -5.8 log η (Pa · s).

Therefore the results from Janz and Saegusa (1963) are not in agreement with the implications of Maxwell theory and the experimental findings of Angell (1989) and seem to be incorrect.

However, in contrast with the results presented in Sato et al. (1999), our viscosity values for Li_2CO_3 are much higher (~3 times) than for Na_2CO_3. This is therefore in

agreement with the theoretical behavior expected for lithium as function of the dimensions of its ionic radius (Sato et al. 1999).

Moreover, in Fig. 5 we plot the calculated viscosities for Na_2CO_3, K_2CO_3 and Li_2CO_3 melts at 1183 K ($10^4/T = 8.5$) as function of the ionic radius of cations.

In doing so, contrary to how reported in Sato et al. (1999) we clearly show that there is a dependency of viscosity on ionic radius of the cation (i.e. viscosity of Li_2CO_3 higher than Na_2CO_3) and confirm that the theoretical predictions of Sato et al. (1999) were correct.

Finally, we investigated the effect of reduced oxygen fugacity (pure CO_2 at 1 bar pressure) on melt viscosity for the sodium carbonate melt (Tab. 2). Before starting the viscosity measurements, the furnace has been previously flushed with a constant CO_2 flow for two hours. Then the target temperature was reached and the viscosity measurements were performed. Fig. 4 shows that, under CO_2 atmosphere, higher viscosity values were measured in respect to those obtained under oxidized conditions (e.g. at 1173 K, η_{air} is 4.7 mPa · s while η_{CO2} is 6.9 mPa · s). This discrepancy in the two values show that reduced conditions have a weak effect on the viscosity of alkali carbonate melts probably due to the different (small) amount of thermodynamically stable alkali oxide in the melt.

Implication and future prospective

Results presented in this study demonstrate the high value of this new adapted rheometric setup in performing high-accuracy and high-precision measurements, with particular emphasis on the rheology of melts at high temperature in general and more

significantly for melts that show extremely low viscosity. The importance of accuracy and precision of the measurements is highlighted by the results obtained on Li-carbonate melts that show for the first time a higher viscosity than Na-carbonate in agreement with the theoretically derived viscosity behavior and validate the predictions of the parameterization proposed by Sato et al. (1999). Our setup discloses future opportunities in expanding the investigated dataset to cover the composition range matching the carbonatite melt chemistry variation observed in nature.

Acknowledgments

We acknowledge the Advanced Researcher Grant of the European Research council (no. 247076; "EVOKES"). C. Cimarelli has been supported by an AXA Research Fund grant. We like to thank J. Läuger, C. Montanaro and S. Kolzenburg for useful discussions. We acknowledge one anonymous reviewer which considerably improve this manuscript.

References

Angell, C.A. (1985) Strong and fragile liquids. In relaxations in complex system, eds K. L. Ngai and G. B. Wright. National technical service US Department of Commerce.

Angell, C.A., Scamehorn, C.A., List, D.J. and Kieffer, J. (1989) Glass forming liquid oxides at the fragile limit of the viscosity-temperature relationship. From Proceedings of XV International Congress on Glass, Leningrad.

Baker, V.R., Komatsu, G., Parker, T.J., Gulick, V.C., Kargel, J.S., and Lewis, J.S. (1992) Channels and valleys on Venus - Preliminary analysis of Magellan data, 97.

Dingwell, D.B. (1986) Viscosity-temparature relationships in the system $Na_2Si_2O_5$-$Na_4Al_2O_5$. Geochimica et Cosmochimica Acta, 50, 1261–1265.

Gaillard, F., Malki, M., Iacono-marziano, G., Pichavant, M., and Scaillet, B. (2008) Carbonatite Melts and Electrical Conductivity in the Asthenosphere. Science, 270, 1363–1365.

Hammouda, T., and Laporte, D. (2000) Ultrafast mantle impregnation by carbonatite melts. Geology, 28, 283–285.

Janz, G.J., and Saegusa, F. (1963) Molten carbonates as electrolytes: viscosity ad transport properties. Journal of the Electrochemical Society, 452–456.

Jones, A.P., Genge, M., and Carmody, L. (2013) Carbonate Melts and Carbonatites. Reviews in Mineralogy and Geochemistry, 75, 289–322.

Kargel, J.S., Kirk, R.L., Fegley, B., and Treiman, A.H. (1994) Carbonate-Sulfate Volcanism on Venus? Icarus, 112, 219–252.

Koishi, T., Kawase, S., Tamaki, S., and Ebisuzaki, T. (2000) Computer simulation of molten Li_2CO_3-K_2CO_3 mixtures. Journal of the Physics Society Japan, 69, 3291–3296.

Läuger, J., and Stettin, H. (2010) Differences between stress and strain control in the non-linear behavior of complex fluids. Rheologica Acta, 49, 909–930.

Liu, Q., Tenner, T.J., and Lange, R.A. (2007) Do carbonate liquids become denser than silicate liquids at pressure? Constraints from the fusion curve of K_2CO_3 to 3.2 GPa. Contributions to Mineralogy and Petrology, 153, 55–66.

Norton, G., and Pinkerton, H. (1997) Rheological properties of natrocarbonatite lavas from Oldoinyo Lengai, Tanzania. European Journal of Mechanics - B/Fluids, 9, 351–364.

Reeve, R.W., and Tseung, A.C.C. (1996) Factors affecting the dissolution and reduction of oxygen in molten carbonate electrolytes. Part 1: Effect of temperature and alkali carbonate mixture. Journal of Electroanalytical Chemistry, 403, 69–83.

Russell, J.K., Giordano, D., and Dingwell, D.B. (2003) High-temperature limits on viscosity of non-Arrhenian silicate melts. American Mineralogist, 88, 1390–1394.

Russell, J.K., Porritt, L.A., Lavallée, Y., and Dingwell, D.B. (2012) Kimberlite ascent by assimilation-fuelled buoyancy. Nature, 481, 352–6.

Sato, Y., Yaegashi, S., Kijima, T., Takeuchi, E., Taman, K., Hasebe, M., Hoshi, M., and Yamamura, T. (1999) Viscosities of molten alkali carbonates. Netsu Bussei, 13, 156–161.

Schmidtke, B., Hofmann, M., Lichtinger, a., Rössler, E. a., (2015). Temperature Dependence of the Segmental Relaxation Time of Polymers Revisited. Macromolecules 48, 3005–3013. doi:10.1021/acs.macromol.5b00204

Shannon, R. D. and Prewitt, C. T. (1969) Effective ionic radii in oxides and fluorides. Acta Crystallographica Section B Structural Crystallography and Crystal Chemistry. 925-946.

Treiman, A. H. (1995) Ca-rich carbonate melts: a regular-solution model, with applications to carbonatite magma + vapor equilibria and carbonate lavas on Venus. American Mineralogist, 80, 115–130.

Vorob'ev G.V., Pal'guev S.F., and Karpachev S.V. (1966) Electrochemistry of molton and solid electrolytes, vol. 3 (ed. A.N. Baraboshrin), p33 (Consultants Bureau).

Yoshiba, F., Morita, H., Yoshikawa, M., Mugikura, Y., Izaki, Y., Watanabe, T., Komoda, M., Masuda, Y., and Zaima, N. (2004) Improvement of electricity generating performance and life expectancy of MCFC stack by applying Li/Na carbonate electrolyte test results and analysis of 0.44 m2/10 kW- and 1.03 m2/10 kW-class stack. Journal of Power Sources, 128, 152–164.

Figure captions

Fig. 1 Sketch of the rheometer and the measuring geometry (concentric cylinder). Additionally, a sketch of the furnace is also shown.

Fig. 2 (a) Measured viscosity of distilled water, as a function of time (min.), at 303 and 333 K. The numbers in the figure show the employed strain rate (sec^{-1}) during the measurements. **(b)** Measured viscosity of silicone standard (Cannon N15000) as a function of time. The measurements were carried out between 298 and 373 K, while the numbers in the figure show the employed strain rate (sec^{-1}) during the measurements.

403 **Fig. 3** Comparison between measured and reference viscosities. The viscosity
404 measurements were performed between 298 and 1273 K, at different shear rates ranging
405 between 0.5 and 70 sec^{-1}. The error is smaller than the symbol size and the 1:1 linear
406 regression agrees to within 0.004 log unit for distilled water, 0.01 log unit for silicone oil
407 standard and 0.02 log unit for DGG-1 standard glass.
408
409 **Fig. 4** Measured viscosity of Li_2CO_3 and Na_2CO_3 as a function of the reciprocal
410 temperature. In the figure it is also shown a comparison between the results obtained in
411 this study and the results presented in Janz and Saegusa (1963) Sato et al. (1999). The
412 error is smaller than the symbol size.
413
414 **Fig. 5** Calculated viscosities for Na_2CO_3, K_2CO_3 and Li_2CO_3 melts at 1183 K ($10^4/T$ =
415 8.5) respect to the ionic radius together with data reported in Sato et al. (1999). The
416 viscosity was calculated using an Arrhenian viscosity–temperature relationship (Eq. 1)
417 and fit parameters reported in Tab. 3. The error is smaller than the symbol size.
418
419 Figure 1

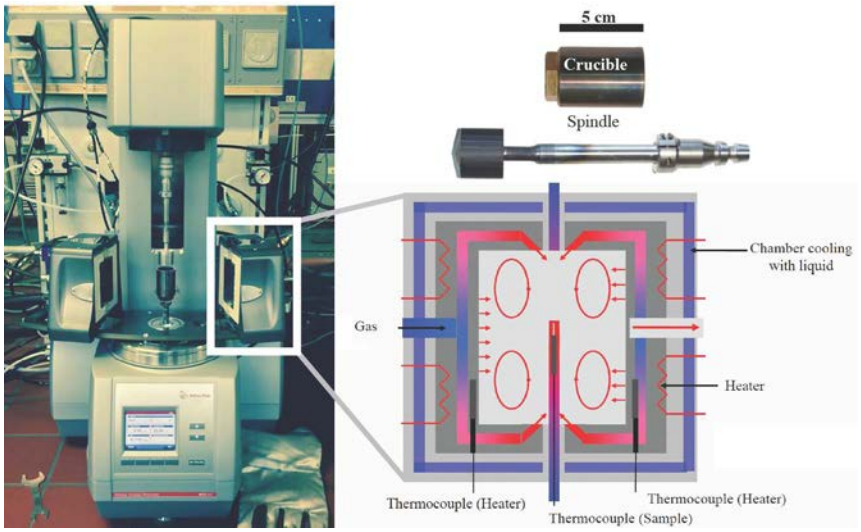

Figure 2

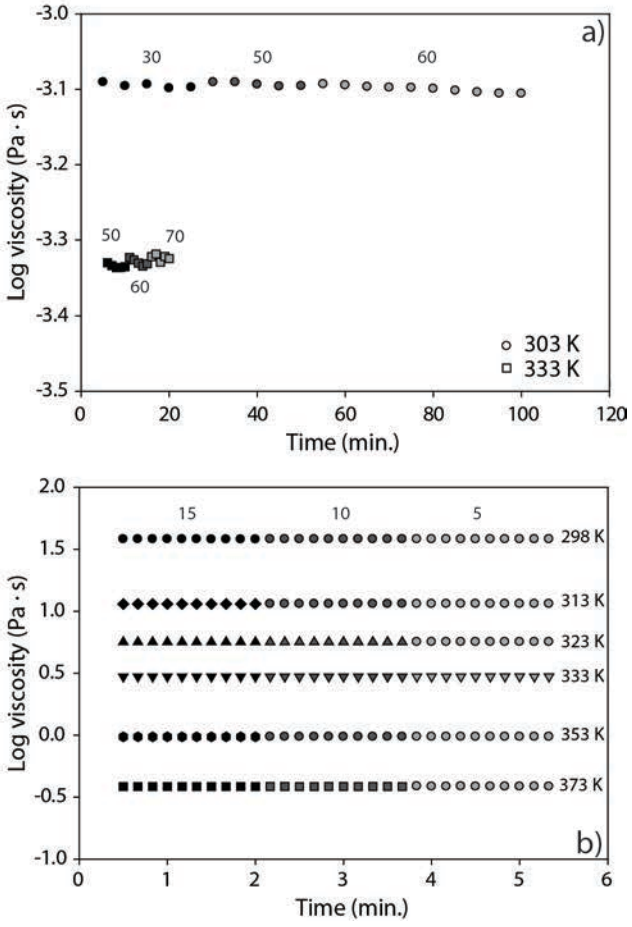

425 Figure 3

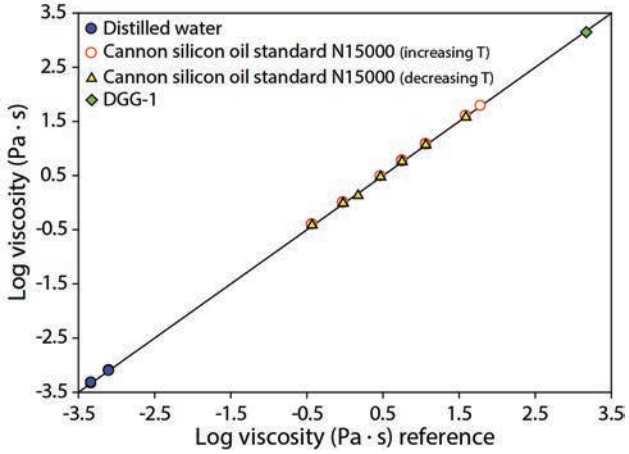

426

427 Figure 4

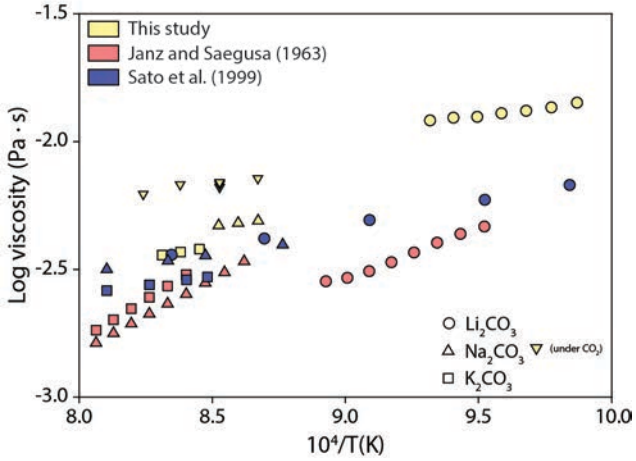

428

429 Figure 5

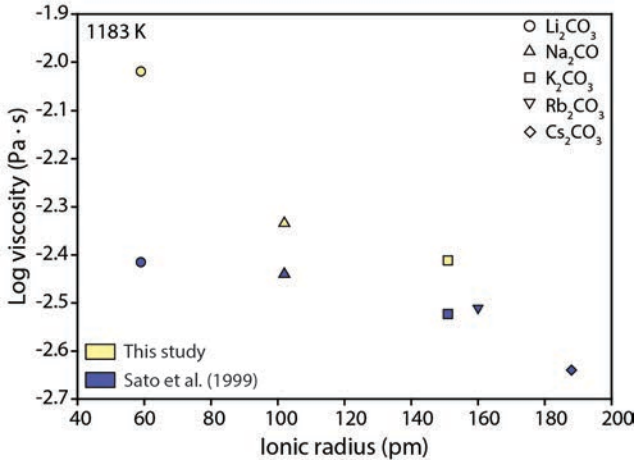

430

Table 1.

Viscosity data from standard materials as a function of temperature and shear rate.

Sample	T (K)	Shear rate (sec^{-1})	Measured log η (Pa · s)	Reference log η (Pa · s)
Distilled water	303	30	-3.095	-3.098
Distilled water	303	50	-3.093	-3.098
Distilled water	303	60	-3.099	-3.098
Distilled water	303	70	-3.105	-3.098
Distilled water	333	30	-3.328	-3.331
Distilled water	333	50	-3.334	-3.331
Distilled water	333	60	-3.328	-3.331
Distilled water	333	70	-3.323	-3.331
Distilled water	333	30	-3.325	-3.331
Distilled water	333	50	-3.335	-3.331
Distilled water	333	60	-3.329	-3.331
Distilled water	333	70	-3.323	-3.331
Cannon N15000	298	15	1.581	1.590
Cannon N15000	298	10	1.581	1.590
Cannon N15000	298	5	1.581	1.590
Cannon N15000	313	15	1.059	1.063
Cannon N15000	313	10	1.059	1.063
Cannon N15000	313	5	1.060	1.063
Cannon N15000	323	15	0.752	0.753
Cannon N15000	323	10	0.752	0.753
Cannon N15000	323	5	0.752	0.753
Cannon N15000	333	15	0.472	0.470
Cannon N15000	333	10	0.472	0.470
Cannon N15000	333	5	0.473	0.470
Cannon N15000	313	15	-0.013	-0.023
Cannon N15000	313	10	-0.013	-0.023
Cannon N15000	313	5	-0.013	-0.023
Cannon N15000	313	15	-0.013	-0.023
Cannon N15000	313	10	-0.013	-0.023
Cannon N15000	313	5	-0.013	-0.023
Cannon N15000	373	15	-0.415	-0.432
Cannon N15000	373	10	-0.415	-0.432
Cannon N15000	373	5	-0.415	-0.432
Cannon N15000	373	15	-0.414	-0.432
Cannon N15000	373	10	-0.414	-0.432
Cannon N15000	373	5	-0.413	-0.432
Cannon N15000	313	15	-0.010	-0.023
Cannon N15000	313	10	-0.009	-0.023
Cannon N15000	313	5	-0.009	-0.023
Cannon N15000	313	15	-0.009	-0.023
Cannon N15000	313	10	-0.009	-0.023
Cannon N15000	313	5	-0.009	-0.023
Cannon N15000	333	15	0.479	0.470
Cannon N15000	333	10	0.479	0.470
Cannon N15000	333	5	0.479	0.470
Cannon N15000	323	15	0.759	0.753
Cannon N15000	323	10	0.760	0.753
Cannon N15000	323	5	0.760	0.753
Cannon N15000	313	15	1.068	1.063
Cannon N15000	313	10	1.069	1.063
Cannon N15000	313	5	1.069	1.063
DGG-1	1273	0.5	3.131	3.173
DGG-1	1273	2.5	3.135	3.173

[a]100* (Measured viscosity – Calculated viscosity)/Calculated viscosity.

Table 2.
Viscosity data from standard materials as a function of temperature and shear rate.

Sample	T (K)	10^4/T (K)	Measured log η (Pa · s)	Measured η (mPa · s)
K_2CO_3	1183	8.5	-2.420	3.80
K_2CO_3	1193[r]	8.4	-2.432	3.70
K_2CO_3	1203[i]	8.3	-2.444	3.60
Na_2CO_3	1153	8.7	-2.310	4.90
Na_2CO_3	1163[r]	8.6	-2.319	4.80
Na_2CO_3	1173[i]	8.5	-2.328	4.70
$Na_2CO_{3\,(CO2)}$	1153	8.7	-2.173	6.71
$Na_2CO_{3\,(CO2)}$	1173	8.5	-2.163	6.87
$Na_2CO_{3\,(CO2)}$	1173	8.5	-2.175	6.68
$Na_2CO_{3\,(CO2)}$	1173	8.5	-2.182	6.58
$Na_2CO_{3\,(CO2)}$	1193	8.4	-2.187	6.50
$Na_2CO_{3\,(CO2)}$	1193	8.4	-2.187	6.50
$Na_2CO_{3\,(CO2)}$	1213[i]	8.2	-2.214	6.11
$Na_2CO_{3\,(CO2)}$	1213[r]	8.2	-2.214	6.11
Li_2CO_3	1013	9.9	-1.848	14.20
Li_2CO_3	1023	9.8	-1.866	13.60
Li_2CO_3	1033	9.7	-1.879	13.20
Li_2CO_3	1043	9.6	-1.889	12.90
Li_2CO_3	1053	9.5	-1.903	12.50
Li_2CO_3	1063[r]	9.4	-1.907	12.40
Li_2CO_3	1073[i]	9.3	-1.917	12.10

[i]first viscosity measurement.
[f]last viscosity measurement.

Table 3.
Fit parameters of experimental data according to the Eq. 1

	A	B	Ionic radius (pm)[a]	E_a (kJ · mol^{-1})
K_2CO_3	-3.83 (0.02)	1671 (21)	151	32.0 (0.4)
Na_2CO_3	-3.37 (0.01)	1224 (13)	102	23.4 (0.3)
Li_2CO_3	-3.05 (0.08)	1216 (83)	59	23.4 (1.6)

[a]Shannon and Prewit (1969).